



Depósito de Investigación
Universidad de Sevilla

Depósito de investigación de la Universidad de Sevilla

<https://idus.us.es/>

“This is an Accepted Manuscript of an article published by Elsevier in SCIENCE OF THE TOTAL ENVIRONMENT on 1 March 2022, available at: <https://doi.org/10.1016/j.scitotenv.2021.151338>”

1 **Maintaining forest cover to enhance temperature buffering under future climate**
2 **change**

3 **Abstract**

4 Forest canopies buffer macroclimatic temperature fluctuations. However, we do not know if and how the
5 capacity of canopies to buffer understorey temperature will change with accelerating climate change. Here
6 we map the difference (offset) between temperatures inside and outside forests in the recent past and
7 project these into the future in boreal, temperate and tropical forests. Using linear mixed-effect models, we
8 combined a global database of 714 paired time series of temperatures (mean, minimum and maximum)
9 measured inside forests vs. in nearby open habitats with maps of macroclimate, topography and forest cover
10 to hindcast past (1970-2000) and to project future (2060-2080) temperature differences between free-air
11 temperatures and sub-canopy microclimates. For all tested future climate scenarios, we project that the
12 difference between maximum temperatures inside and outside forests across the globe will increase (i.e.
13 result in stronger cooling in forests), on average during 2060-2080, by 0.27 ± 0.16 °C (RCP2.6) and 0.60 ± 0.14
14 °C (RCP8.5) due to macroclimate changes. This suggests that extremely hot temperatures under forest
15 canopies will, on average, warm less than outside forests as macroclimate warms. This knowledge is of
16 utmost importance as it suggests that forest microclimates will warm at a slower rate than non-forested
17 areas, assuming that forest cover is maintained. Species adapted to colder growing conditions may thus find
18 shelter and survive longer than anticipated at a given forest site. This highlights the potential role of forests
19 as a whole as microrefugia for biodiversity under future climate change.

20 **Keywords:** forest microclimate, temperature offsets, canopy, climate change, future
21 climate projections, paired sensor data

22

23 **Introduction**

24 Warming temperatures and changing precipitation regimes are influencing ecosystems across the globe
25 (IPCC, 2018). To date, ecological research assessing the impact of anthropogenic climate change has
26 predominantly relied on macroclimatic data. These data are typically based on a global network of weather
27 stations established at approximately 1.5 to 2.0 m above the soil surface in open habitats (e.g. above short
28 grass) (World Meteorological Organization, 2018). Forest organisms living below and within tree canopies,
29 however, experience microclimatic conditions distinct from those in open habitats (Chen et al., 1999; De
30 Frenne et al., 2021; Geiger et al., 2009). Below tree canopies, lower radiation, wind and evapotranspiration
31 rates often translate into lower temporal variation in air temperature and humidity compared to open
32 environments (Davis et al., 2019; Geiger et al., 2009; Von Arx et al., 2013). In particular, temperature
33 extremes are often strongly attenuated in forest interiors, with lower maxima and higher minima compared
34 to open environments (De Frenne et al., 2019; Li et al., 2015). Studies have already shown that such
35 microclimatic buffering can mediate the response of forest communities to climate change (De Frenne et al.,
36 2013; Dietz et al., 2020; Lenoir et al., 2017; Stevens et al., 2015; Zellweger et al., 2020). Despite the increasing
37 evidence that ecosystem dynamics and processes are more likely to be related to forest microclimates than
38 to macroclimate (Chen et al., 2018; De Frenne et al., 2021; De Smedt et al., 2021; Frey et al., 2016a),
39 microclimates are still seldom incorporated in ecological research (e.g. in species distribution models)
40 (Lembrechts et al., 2019) and ignored by dynamic global vegetation models (DGVMs; e.g. Thrippleton,
41 Bugmann, Kramer-Priewasser, & Snell, 2016) that simulate the effects of future climate change on natural
42 vegetation and its carbon and water cycles. In particular, we do not know how forest microclimates will
43 change in the future as macroclimate changes (Lembrechts and Nijs, 2020).

44 Advances in studies on the effects of climate change on different organisms living below or in forest canopies
45 have often been limited by the availability of suitable microclimatic data (De Frenne et al., 2021). One robust
46 way to study forest microclimates is to use microclimate measurements from paired (inside vs. outside
47 forests) sensor networks to calculate temperature offsets, i.e. the absolute and instantaneous difference
48 between temperature inside (i.e., microclimate) and free-air temperatures outside forests (i.e.,

49 macroclimate) (*sensu* De Frenne et al., 2021). Negative offset values thus reflect cooler and positive offsets
50 warmer forest temperatures compared to outside forests. These empirical offset values for temperature can
51 be related to readily available environmental data using statistical modelling approaches, and these models
52 can then be used to interpolate and extrapolate microclimate across entire mapped landscapes (Frey et al.,
53 2016b; Greiser et al., 2018). Differences between macro- and microclimate (i.e., temperature offsets) result
54 from processes operating at many scales that influence incoming solar radiation, air mixing, soil properties
55 or evapotranspiration (reviewed in De Frenne et al., 2021). Macroclimatic conditions (e.g., mean temperature
56 and rainfall), topographic variation in the landscape (e.g., elevation and aspect) and variation in canopy cover
57 and vegetation height have been reported to be the main drivers of the understory temperatures in forests
58 (De Frenne et al., 2021, 2019; Greiser et al., 2018; Macek et al., 2019; Zellweger et al., 2019). With the advent
59 of global forest microclimate data (De Frenne et al., 2019; Zellweger et al., 2020), this type of modelling now
60 enables the prediction of forest microclimates across forest types under future climate change.

61 Here we map forest microclimate temperature offsets based on (i) paired sensor measurements below the
62 canopy vs. the open-air temperature at a given site and (ii) landscape- and canopy-scale predictors
63 throughout the year for the Earth's dominant forested ecosystems across five continents and at a spatial
64 resolution of ~1 km. More specifically, our objectives were to (1) make predictions for mean, minimum and
65 maximum temperatures using past macroclimatic data (1970-2000), and, (2) make projections for
66 temperature offsets for the future (2060-2080) macroclimatic conditions. We hypothesised that the
67 buffering capacity of forest canopies results in slower future warming of forest below-canopy temperatures
68 compared to the warming observed in standard meteorological weather stations (macroclimate).

69

70 **Material & Methods**

71 **Paired plot data**

72 We used a unique data set with 714 temperature offset data points involving paired plots from 74 studies
73 spread across 5 continents (Supplementary Material Fig. S1; Data available in De Frenne et al., 2019). Focus
74 was on air temperature below tree canopies (~72% of observations) and the temperature of the topsoil
75 (~28%), given their importance for responses of forest organisms and ecosystem functioning to macroclimate
76 warming. A key asset of this database is the paired nature of the data, which always combines below-canopy
77 temperature data at a given forest site with open-air temperature data from a neighbouring reference non-
78 forest site. Temperature measurement were performed by various logger types such as HOBO loggers (~15%
79 of observations), iButton loggers (~10%), full weather stations (~5%) and various other logger types (e.g.
80 cylindrical thermistor, Hanna thermohygrometer, thermocouples, etc.; ~70%). Reference sites were a nearby
81 open site equipped with the same type of (shielded) temperature loggers (~82% of observations), a nearby
82 weather station (~14%) (provided the distance did not conflict with the temperature offset of the canopy,
83 e.g., due to significant topographic differences) or a logger placed above the upper canopy surface (~4%). We
84 specifically refrained from using additional data on forest microclimate conditions that were not strictly
85 paired with free-air conditions from a neighbouring site using the exact same design (same sensor, same
86 logger, same shielding material, same height).

87 The data points were collated from the scientific literature in a systematic and reproducible manner (see De
88 Frenne et al., 2019 for full details). Temperature offsets were calculated as the temperature inside the forest
89 minus the temperature outside the forest, or extracted directly from the original study; negative values
90 reflect cooler temperatures below tree canopies while positive values reflect warmer understorey
91 temperatures. This was done for three temperature response variables, i.e. mean, maximum, and minimum
92 temperature (further referred to as T_{mean} , T_{min} and T_{max} , respectively) that were computed during a specific
93 time period that could differ between sites but that was exactly the same between paired sensors installed
94 outside and inside the forest at a given site. Multiple forest sites (at least several kilometres apart), seasons
95 (meteorological seasons, later aggregated to growing versus non-growing season) and temperature metrics

96 (maximum, mean, minimum, air or soil temperatures) originating from the same study were entered into
97 different rows of the database but tagged under the same study ID. Temperature values of long time series
98 were always aggregated per season and/or year, which means that several temperature values for T_{mean} , T_{min}
99 or T_{max} could be generated for the same study site. Temperature measurements were classified as having
100 taken place during the growing season, the non-growing season or throughout the whole year. This
101 classification was performed on the basis of reported meteorological seasons and/or climate information in
102 the original study. The dry and winter season were classified as the non-growing season in tropical and
103 temperate biomes, respectively. Estimates of uncertainty (standard error, standard deviation, coefficient of
104 variation or confidence intervals) of the temperature measurements were only reported for a small minority
105 (13.6%) of offset values in the database and were thus not included in our analyses. See De Frenne et al.
106 (2019) for more details on the literature search, inclusion criteria and the empirical data used in this study.

107 **Predictor variables**

108 To predict the offsets for the three temperature variables (T_{mean} , T_{max} , T_{min}) across all forests at a global extent,
109 we gathered global maps of predictor variables related to macroclimate, topography and forest cover. These
110 three sets of predictor variables were selected based on their importance for forest microclimate, and on the
111 spatial resolution and extent of the available data. All the predictor maps we used are raster maps with a
112 spatial resolution of 30 arcsec (~1 km) and are available at the global extent (i.e., from 80°N to 56°S in latitude
113 and from 180°E to 180°W in longitude). Values for all predictor variables were extracted using the
114 geographical coordinates for each plot pair.

115 *Macroclimate.* Global raster maps of mean, minimum and maximum free-air temperature (°C; T_{macro}),
116 on a monthly basis, as well as monthly precipitation (mm) raster maps, averaged for the climatology
117 1970-2000, were collected from WorldClim version 2.1 (Fick and Hijmans, 2017). In addition, we
118 gathered future projections (2060-2080) for the exact same set of temperature and precipitation
119 variables described in the previous sentence but based on the contrasting “very stringent”
120 representative concentration pathway (RCP) 2.6 and “worst case” RCP 8.5 from three different
121 general circulation models (GCMs) with minimal interdependency, based on Sanderson et al. (2015),

122 i.e. HadGEM2-ES, MPI-ESM-LR and MIROC5 (downscaled CMIP5 data from WorldClim; 30 arcsec
123 resolution).

124 *Topographic variables and distance to the coast.* We gathered six variables related to topography
125 using raster layers derived from the Global Multi-resolution Terrain Elevation Data 2010
126 (GMTED2010) dataset at 30 arcsec resolution (Amatulli et al., 2018). Maps on northness and
127 eastness, elevation (m a.s.l.), elevational variation (EleVar) and topographic position index (TPI) were
128 collected. Northness and eastness are the sine of the slope, multiplied by the cosine and sine of the
129 aspect, respectively. They provide continuous measures describing the orientation in combination
130 with the slope (i.e., a circular variable is transformed into a continuous one, ranging from -1 to 1). In
131 the Northern Hemisphere, a northness value close to 1 corresponds to a northern exposition on a
132 vertical slope (i.e., a slope exposed to very low amount of solar radiation), while a value close to -1
133 corresponds to a very steep southern slope, exposed to a high amount of solar radiation. Aspect
134 values for the Southern Hemisphere were inverted so that a value of 1 in the Southern Hemisphere
135 also means very low amount of solar radiation. Variables EleVar (1) and TPI (2) capture topographic
136 heterogeneity within a 1 km² grid cell around each pair of measurements (inside and outside forest):
137 (1) the standard deviation of elevational values aggregated per 1 km² grid cell (further referred to as
138 elevational variation) and (2) the median of the topographic position index (TPI) values across each
139 1 km² grid cell. The TPI is the difference between the elevation of a focal cell and the mean elevation
140 of its eight surrounding cells. Positive and negative values correspond to ridges and valleys,
141 respectively, while zero values correspond to flat areas (Amatulli et al., 2018). We also produced a
142 map with the distance from each land pixel to the nearest coastline (Dist2Coast) using the coastline
143 map data from Natural Earth (free vector data from naturalearthdata.com).

144 *Forest cover and forest height.* We used the tree canopy cover (defined as canopy closure for all
145 vegetation taller than 5 m in height) map for the year 2000 by Hansen et al. (2013). This high-
146 resolution global map layer was re-projected and aggregated from 30 m to 30 arcsec using the
147 average of the aggregated raster cells. This canopy cover map is the only available map spanning a
148 global extent at this high resolution. By using this data product, we make the strong assumption that

149 canopy cover at the time of temperature measurements is similar to the cover in the year 2000. We
150 consider this assumption as reasonable as the median year of the temperature measurements for all
151 data points is approximately 1996 (range between 1943 and 2014). Finally, we used estimates of
152 canopy height at 1 km resolution derived from the ICESat satellite mission based on 2005 (Simard et
153 al., 2011).

154 **Data analysis**

155 All statistical analyses were performed in the open-source statistical software environment of R, version 4.0.2
156 (R Core Team, 2021). The temperature offsets for T_{mean} , T_{max} and T_{min} were modelled (274, 184 and 202 plot
157 pairs respectively), after removing missing values for sensor height, i.e. not mentioned in the original study,
158 and data points with canopy cover zero (based on the tree canopy cover map introduced above; Hansen et
159 al., 2013) using linear mixed-effect models with random intercept (LMMs) (*lme4* package; Bates et al., 2015).
160 In our main models, we combined the seasonal (growing vs. non-growing and annual) time series and
161 performed additional analyses for the different three different time periods (see further and Supplementary
162 Material Appendix S2). We included 'study ID' as a random intercept term to account for non-independence
163 between samples within studies. For each of the three studied response variables, we started our modelling
164 protocol from the full model:

165 $T_{\text{offset}} \sim T_{\text{macro}} + \text{Precipitation} + \text{Elevation} + \text{Eastness} + \text{Northness} + \text{EleVar} + \text{TPI} + \text{Dist2Coast} + \text{Canopy cover} +$
166 $\text{Forest height} + \text{Sensor height} + \text{random effect 'study ID'}$

167 For T_{macro} , we used the monthly average for either T_{mean} , T_{max} and T_{min} temperature during the period 1970-
168 2000 depending on the studied response variable of T offset (T_{mean} , T_{max} or T_{min}). Sensor height was also
169 included in the models (continuous variable, in metres above or below the soil surface), as this significantly
170 impacts the magnitude of the temperature offset (De Frenne et al., 2019; Supplementary Fig. S2; Table S1).
171 Sensor height is positive for aboveground and negative for belowground sensors. Data points with sensor
172 height > 2 m were excluded as our aim was to model forest microclimate near the ground. To avoid
173 collinearity in predictor variables and improve model performance, we excluded variables that showed a
174 correlation $r \geq |0.7|$ (Pearson's product-moment correlation; Supplementary Fig. S3) and variance inflation

175 factor ≥ 4 (Zuur et al., 2010). Forest height was therefore removed from all models due to high correlation
176 with canopy cover; for T_{mean} offset, EleVar was also dropped from the model due to high correlation with TPI.
177 All predictors were standardized by subtracting the mean and dividing by the standard deviation prior to
178 modelling. For each response variable, the single best model was selected based on the Akaike Information
179 Criterion (AIC) using the automated dredge-function of the package MuMIn (Barton, 2009). Goodness of fit
180 was calculated following Nakagawa and Schielzeth (2013).

181 To test for non-linear relationships, we also used generalized additive mixed-effect models (GAMMs) (cf. the
182 *gamm4* package) (Wood and Scheipl, 2014) on the same dataset. We applied smoothers to the same set of
183 fixed-effect terms, included the same random intercept term 'study ID' and followed the same model
184 selection procedure as for the LMMs. For each of the three studied response variables (T_{mean} , T_{max} , T_{min}) and
185 for each of the two modelling approaches, we performed a leave-one-out cross validation (LOOCV) and
186 compared root mean square errors (RMSE) among models (LMMs vs. GAMMs). We found no difference (t
187 test, p-value > 0.05) in RMSE between LMMs and GAMMs, justifying our choice of LMMs (see also
188 Supplementary Fig. S4). Furthermore, we checked spatial autocorrelation in the model residuals for the
189 LMMs using Moran's I-test from the *ape* package (Paradis and Schliep, 2019). No spatial autocorrelation was
190 detected (p-value > 0.05) in the model residuals. Additionally, we tested the effect of season of sampling
191 (annual, growing and non-growing season; see above) on each response variable. We included season as a
192 categorical variable to the full models described above and followed the same model selection procedure.
193 However, due to the low number of observations for each category (but growing season being the dominant
194 category), results including season were only included in the Supplementary Material Appendix S2.

195 Using the single best LMMs for each of our three response variables, we made predictions for T_{mean} , T_{max} , and
196 T_{min} offsets for forest across the globe using the collected map data for all predictor variables retained in the
197 models, setting sensor height to 1.0 m and not considering variation included in the random intercept.
198 Temperature offsets were predicted for all raster pixels (30 arcsec resolution) with canopy cover $>50\%$ as this
199 largely concurs with the global distribution of forest areas in the terrestrial ecoregions map by Olson et al.
200 (2001). To assess model performance, we performed spatially blocked k-fold cross-validation ($k = 10$; folds
201 assigned randomly, with spatial blocks of size 50 km²; Valavi et al., 2019). Furthermore, we made predictions

202 of future forest temperature offsets based on the future projections of temperature and precipitation (the
203 latter only included in the best model for T_{mean} and T_{min}) from WorldClim (see above). We made future
204 predictions for the period of 2060-2080 using the RCP 2.6 and RCP 8.5 projections based on the three selected
205 GCMs to account for uncertainty related to the GCMs; final model predictions for each RCP scenario were
206 averaged over all GCMs. For the future predictions, we assumed no change in topography and conservatively
207 assumed no change in canopy cover as our main goal was to determine direct climate change effects on
208 temperature offsets below forest canopies if we maintain the forest cover. Of course, we could use different
209 scenarios of future forest cover but we decided to not do that to better assess the unique effect of future
210 climate change without changing other parameters, such as forest cover, in the model. Besides, future
211 scenario on forest cover are not yet available at a global extent and at the spatial resolution we used here.
212 Uncertainty in predictions was mapped by applying a bootstrap approach. We resampled the original data
213 used to fit the models with replacement with total size of the bootstrap samples equal to the size of the
214 original sample. For each of the temperature responses, we fitted single best models using 30 bootstrap
215 samples. Using these 30 models, we generated per-pixel standard deviation mapped at the global extent
216 (Supplementary Fig. S5). To map uncertainty for the future predictions, the same procedure was followed for
217 each of the three GCMs, i.e. 30 bootstraps per GCM. Furthermore, we provide maps indicating where the
218 models are extrapolating beyond the values of data used to fit the models. Predictive performance and
219 uncertainty mapping were performed considering fixed effects of the models, excluding uncertainty of the
220 random (study) effects. Predictions were made using the *raster* package (Hijmans and van Etten, 2012).
221 Graphical plots were created using *ggplot2* (Wickham, 2016) and *Tmap* packages (Tennekes, 2018).

222 **Results**

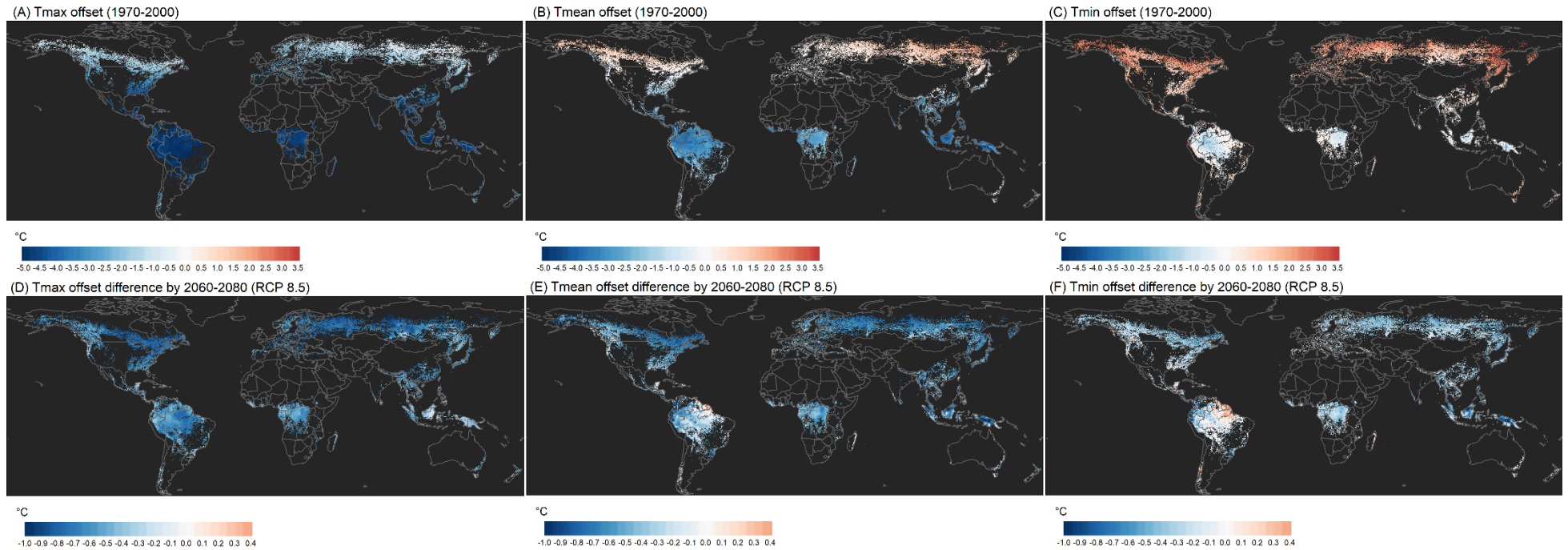
223 Our models predicted an average global offset of -2.92 ± 1.57 °C (mean \pm SD) for T_{max} , -0.88 ± 1.82 °C for T_{mean} ,
224 and 0.96 ± 1.27 °C for T_{min} (Fig. 1 and 2). These averages were calculated from all pixels having at least 50%
225 canopy cover during the year 2000 (Hansen et al., 2013) and derived from the predictions in Fig. 1. Our
226 predictions show a slightly positive T_{mean} offset (i.e. warmer temperatures within the forest) in boreal forests,
227 becoming overall negative towards the tropics (i.e. cooler temperatures within tropical forests compared to

228 free-air temperatures) (left panels Fig. 2). T_{\max} offsets are negative across the three biomes (i.e. cooler
229 maximum temperatures within forests) with the lowest values in the tropics (up to 5 degrees cooler within
230 forests), whereas T_{\min} offsets are positive in boreal and temperate forests and negative in the tropics (Fig. 2).
231 When including season in the modelling procedure, we found that for T_{mean} offsets were lower during the
232 growing season than for the non-growing season across the three biomes. For T_{\max} and T_{\min} , season was not
233 included in the best model (more detailed results included in Supplementary Material Appendix S2).

234 Offsets for T_{\max} , T_{mean} and T_{\min} were negatively affected by free-air, macroclimate temperatures
235 (Supplementary Fig. S2 and Table S1). For T_{mean} and T_{\min} , we found lower offset values with higher amounts
236 of precipitation (Supplementary Fig. S2 and Table S1), for T_{mean} this indicates stronger buffering (more
237 negative offsets), whereas for T_{\min} this means weaker buffering (offsets closer to zero). We found T_{\min} offsets
238 to be more positive, i.e. more strongly buffered, in areas with higher canopy cover, on pole-facing slopes and
239 closer to the coast. The marginal R^2 values (for fixed effects) were 0.29 (0.03 SD), 0.21 (0.03 SD) and 0.25
240 (0.03 SD), while conditional R^2 values (for fixed and random effects) reached 0.58 (0.04 SD), 0.60 (0.06 SD)
241 and 0.52 (0.04 SD) for T_{\max} , T_{mean} and T_{\min} , respectively. Root mean square errors obtained from the spatial
242 cross-validation were 3.67 °C (1.55 SD), 1.78 °C (0.71 SD) and 1.52 °C (0.45 SD) for T_{\max} , T_{mean} and T_{\min} ,
243 respectively. Standard deviations obtained from the bootstrapping procedure show fair consistency between
244 the predictions of the 30 bootstrapped models (Supplementary Table S2; Fig. S5 and S6). Upper confidence
245 levels (95%) of standard deviations for all three responses remained lower than 1 °C (Supplementary Table
246 S2 and Fig. S6). Higher values were mainly observed in the tropical and boreal region. We also found higher
247 extrapolation for the predictors included in the models in tropical forests and especially in the boreal region
248 (Supplementary Fig. S7).

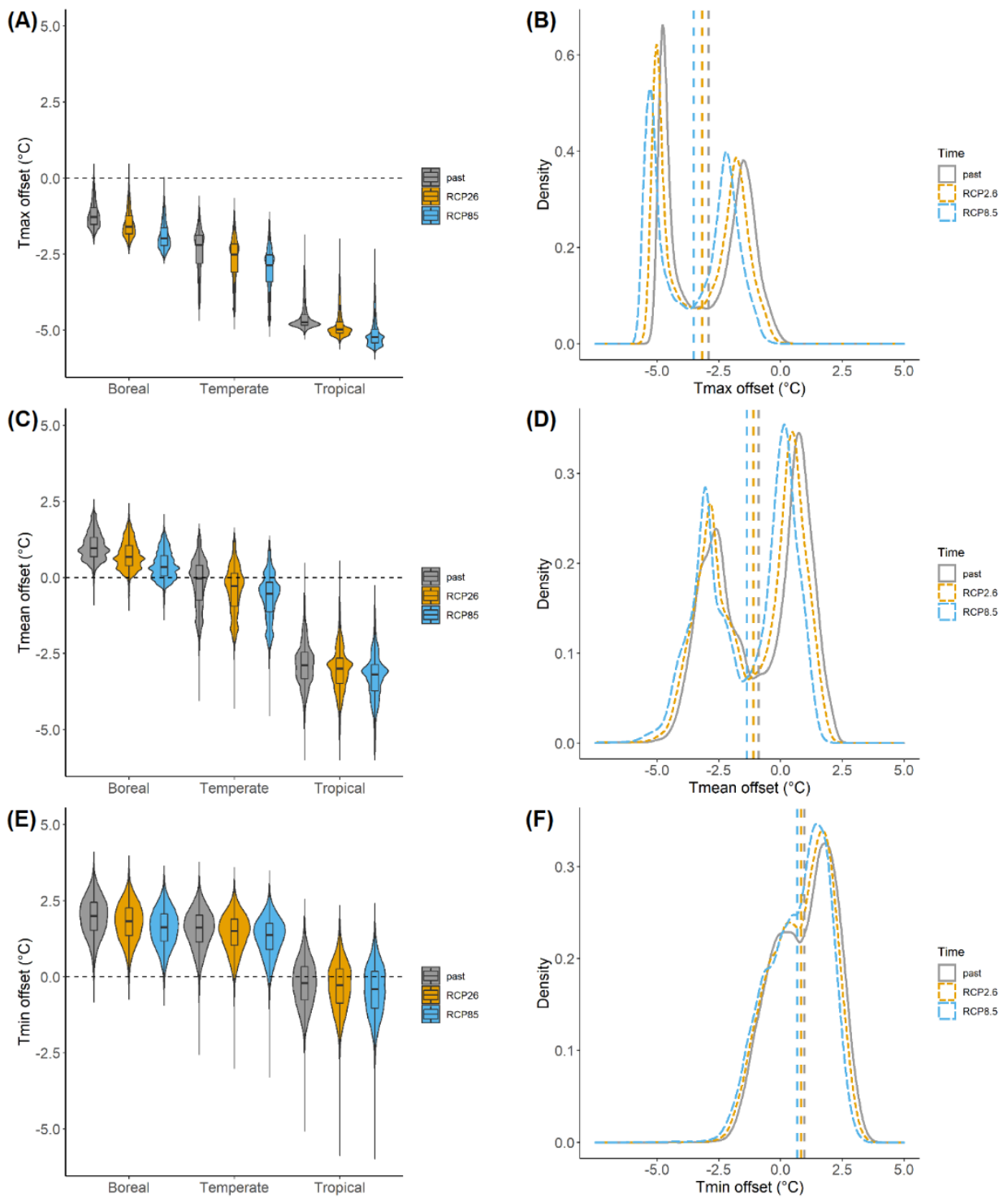
249 Our future projections showed an overall decrease in offset values for all three temperature responses (Fig.
250 2). For T_{mean} , future minus past offsets were -0.22 ± 0.16 °C (mean + SD) for RCP2.6 and -0.5 ± 0.22 °C for
251 RCP8.5 (Fig. 2). For T_{\max} , future minus past offsets were -0.27 ± 0.16 °C for RCP2.6 and -0.60 ± 0.14 °C for
252 RCP8.5 (i.e. cooler maximum temperatures within forests compared to outside temperatures in the future).
253 For T_{\min} , future minus past offsets were -0.12 ± 0.18 °C for RCP2.6 and -0.27 ± 0.24 °C for RCP8.5. These
254 averages were derived from panels D, E and F in Fig. 1. For both T_{\max} and T_{mean} , this means stronger offsets or

255 buffering (more negative offsets), whereas for T_{\min} weaker buffering (offsets closer to zero). Decreases in T_{\min}
256 offsets are most pronounced in the boreal and temperate region (left panels Fig. 2).



257

258 Fig. 1. First row: Global maps of past (1970-2000 climate) forest temperature offsets of (A) maximum, (B) mean and (C) minimum temperatures below tree canopies. Second row:
 259 Maps showing the difference between (D) maximum, (E) mean and (F) minimum temperature offset predictions based on future climatic conditions under RCP8.5 scenarios and past
 260 (1970-2000) offsets (future minus past, negative values thus depict lower offsets in the future than in the recent past which mean higher buffering for T_{max} and T_{mean} but lower for
 261 T_{min}). Predictions were made based on linear mixed-effects models and only for pixels where the canopy cover in the year 2000 is > 50% (Hansen et al., 2013).



262

263 Fig. 2. Left panels: Violin and box plots showing the distribution of predicted below-canopy forest temperature offsets
 264 of (A) T_{max} , (C) T_{mean} , and (E) T_{min} across boreal, temperate and tropical forests classified following Olson et al. (2001).
 265 Right panels: density plots for the predicted offsets of (B) T_{max} , (D) T_{mean} , and (F) T_{min} . Dashed vertical lines represent
 266 global mean offset values for the three temperature responses for past, and the future RCP2.6 and RCP8.5 scenarios.
 267 Note that bimodality is observed in the density plots, resulting from the difference between offsets in temperate and
 268 boreal versus tropical forests (see Fig. 1). For all plots, different colours and line types represent predictions for past
 269 climatic conditions (macroclimate temperature and precipitation, grey), for RCP2.6 (orange) and RCP8.5 scenarios
 270 (blue). Data points to draw these plots are subsamples (10^5 pixels) derived from the global predictions in Fig. 1.

271

272

273 Discussion

274 Our predictions of temperature offsets for the 1970-2000 climatology and for forests having at least 50% tree
275 cover during the year 2000 (Hansen et al., 2013) show that mean temperatures are on average cooler below
276 canopies (at 1 m height) than in open habitats across all forested grid cells (De Frenne et al., 2019; Li et al.,
277 2015). Our results also support the fact that temperature extremes are mainly buffered in forests; T_{\max} is on
278 average lower inside forests, whereas T_{\min} is warmer. Nevertheless, strong biome-specific variation was
279 observed: while in boreal forests, T_{mean} offsets were slightly positive, they became overall negative towards
280 the tropics. T_{\max} offsets were negative across the three biomes with the most negative values in the (warmer)
281 tropics, whereas T_{\min} offsets were positive in the cooler boreal and temperate forests, and negative in the
282 warm tropics. Furthermore, the difference between growing and non-growing season on T_{mean} offsets
283 illustrates the importance of considering the temporal and seasonal variation in temperature offsets in future
284 research (Li et al., 2015; Zellweger et al., 2019).

285 Temperature offsets for all three responses were negatively related to macroclimate temperatures. This
286 relationship is expected as temperature offsets are directly linked to macroclimate temperatures; if free-air
287 temperatures rise, offsets will become more negative because the parameter estimate for T_{macro} represents
288 the proportional buffering of canopies of free-air temperatures. Offsets for T_{mean} and T_{\min} were negatively
289 affected by precipitation. That is, the buffering for T_{\max} by canopies was stronger in regions with higher
290 amounts of precipitation, whereas buffering is lower for T_{\min} , supporting the notion that evapotranspiration
291 drives the offset in these conditions (Davis et al., 2019). The limited role of drivers other than macroclimate
292 could be because the 30 arcsec (~ 1 km) spatial resolution is still too coarse to detect effects of e.g. topography
293 or canopy cover, drivers acting on a very local scale (Ashcroft and Gollan, 2012; Greiser et al., 2018; Macek
294 et al., 2019).

295 Our aim was not to produce maps for use, but to give an overview of how temperature offsets between
296 forest and open habitats vary across forest biomes and how these relationships can evolve under climate
297 change. Despite the limitations of the data and the assumptions made, we found that our models explained
298 a moderately large amount of variation in the offsets, and considered model accuracy to be fair. Uncertainty

299 in predictions increased towards tropical and boreal forests which is likely caused by extrapolation outside
300 the environmental range included in our data. These biomes were underrepresented in the data, hence,
301 future research should focus on setting out networks of paired temperature sensors in these regions
302 (Lembrechts et al., 2021b).

303 Our projections for both the “very stringent” RCP2.6 as well as the “worst-case” RCP8.5 scenario indicate
304 that buffering by forest canopies for T_{mean} and T_{max} temperature may increase, but minimum temperature
305 offsets will decrease, especially in temperate and boreal regions as ambient temperatures become less cold.
306 This suggests that under climate change, free-air temperatures are likely to have a larger-magnitude increase
307 than the corresponding forest microclimate temperatures, which would reinforce the idea of divergent
308 warming (decoupling) between macroclimate and microclimate (De Frenne et al., 2019; Lenoir et al., 2017).
309 Offsets may even become lower (resulting in increasing or decreasing buffering for T_{mean} or T_{min} , respectively)
310 despite projected decreases in precipitation in some regions (Supplementary Fig. S8). It is possible that finer-
311 grained microclimatic heterogeneity could buffer the impact of a changing macroclimate even further
312 (Maclean et al., 2017). This inference relies, however, on the strong assumption that forest cover and
313 composition will remain stable in the future. Such stability is however unlikely, as climate change itself as
314 well as forest management and disturbances can either increase or decrease forest canopy cover in the
315 future. For example, climate change is however likely to cause increased tree mortality owing to, for instance,
316 repeated and more severe disturbances such as droughts, fires, pathogens and insect outbreaks (Curtis et
317 al., 2018; Senf et al., 2021; Senf and Seidl, 2020). The resulting reduction in tree canopy cover can lead to a
318 sudden loss (i.e. a tipping point) of canopy buffering and increased microclimate warming (Alkama and
319 Cescatti, 2016; Findell et al., 2017; Lembrechts and Nijs, 2020; Richard et al., 2021; Zellweger et al., 2020).
320 On the other hand, strong efforts are being made worldwide to increase forest cover and implement climate-
321 smart forestry practices (Bastin et al., 2019; Di Sacco et al., 2021). How these forest cover changes will affect
322 future forest temperature buffering should be a topic for future forest microclimate research.

323 We projected temperature buffering capacities of forests across the globe under future climate change
324 scenarios. Assuming no change in forest composition, we predicted that forest buffering of T_{mean} and T_{max} will
325 increase in the future (2060-2080), whereas buffering of T_{min} will be reduced due to changes in macroclimate

326 conditions. Our results indicate that the refugial capacity of cool and dense forest might last longer than
327 anticipated in a warming climate. This knowledge has important implications for forest biodiversity
328 conservation. Forest managers and policymakers could, for example, aim to optimise forest functioning and
329 biodiversity goals by identifying areas in which reducing or retaining canopy cover may have larger impacts
330 on the prevailing microclimate than anticipated under future climate change (Wolf et al., 2021). The paired
331 nature of the data allowed us to model absolute temperature offsets across a global extent with fair accuracy.
332 Gridded microclimate products such as ours, especially when paired with new, well-designed networks of
333 microclimate measurements (Lembrechts et al., 2020) serve ecological and environmental modelers with a
334 more scale-relevant set of products for making predictions and drawing inference. At the regional and even
335 continental scale, novel high-resolution data on forest structure and composition based on remote sensing
336 imagery (e.g. GEDI LiDAR data) are becoming available (De Frenne et al., 2021; Lembrechts et al., 2019;
337 Randin et al., 2020; Zellweger et al., 2018). Including these microclimate measurements and novel spatial
338 map data (e.g. Haesen et al., 2021; Lembrechts et al., 2020) in future models and mapping efforts will increase
339 accuracy of future predictions (Lembrechts et al., 2021a). Our study illustrates that forest microclimates
340 themselves are subject to climate change, which will have important consequences for forest-dwelling
341 species and must hence not be neglected.

342 **Data availability:**

343 The dataset analysed in the current study is available in the Figshare repository, with the identifier
344 10.6084/m9.figshare.7604849 (de Frenne et al., 2019).

345 **Acknowledgements:**

346 EDL, PV, PDF, LD, PS, CM and TV received funding from the European Research Council (ERC) under the
347 European Union's Horizon 2020 research and innovation programme (ERC Starting Grant FORMICA 757833).
348 FZ received funding from the Swiss National Science Foundation (grant number 193645). SH received funding
349 from a FLOF fellowship of the KU Leuven (project nr. 3E190655). Funding for DHK was provided by the
350 National Science Foundation Graduate Research Fellowship Program (DGE-1842473). JA acknowledges
351 Academy of Finland Flagship funding (grant no. 337552). KH received funding from the Swedish Research
352 Council Formas (grants 2014-530 and 2018-2829) and the Bolin Centre for Climate Research, Stockholm
353 University. SG was supported by the Research Foundation Flanders (FWO) (project G0H1517N). JLL received
354 funding from the Research Foundation Flanders (FWO) (project 12P1819N). JL received funding from the
355 Agence Nationale de la Recherche (ANR) within the framework of the IMPRINT project "Impacts des

356 PProcessus microclimatiques sur la redistributioN de la biodiversité forestière en contexte de réchauffement
357 du macroclimat” (grant number: ANR-19-CE32-0005-01). KDP received funding from the Research
358 Foundation Flanders (FWO) (project ASP035-19). FRS was supported by the VI Plan Propio de Investigación
359 of Universidad de Sevilla (VI PPIT- US).

360

361

362 **References**

- 363 Alkama, R., Cescatti, A., 2016. Climate change: Biophysical climate impacts of recent changes in global
364 forest cover. *Science* (80-). 351, 600–604. <https://doi.org/10.1126/science.aac8083>
- 365 Amatulli, G., Domisch, S., Tuanmu, M.N., Parmentier, B., Ranipeta, A., Malczyk, J., Jetz, W., 2018. Data
366 Descriptor: A suite of global, cross-scale topographic variables for environmental and biodiversity
367 modeling. *Sci. Data* 5, 1–15. <https://doi.org/10.1038/sdata.2018.40>
- 368 Ashcroft, M.B., Gollan, J.R., 2012. Fine-resolution (25 m) topoclimatic grids of near-surface (5 cm) extreme
369 temperatures and humidities across various habitats in a large (200 × 300 km) and diverse region. *Int.*
370 *J. Climatol.* 32, 2134–2148. <https://doi.org/10.1002/joc.2428>
- 371 Barton, K., 2009. MuMIn: Multi-Model Inference.
- 372 Bastin, J., Finegold, Y., Garcia, C., Mollicone, D., Rezende, M., Routh, D., Zohner, C., Crowther, T., 2019. The
373 global tree restoration potential. *Science* (80-). 365, 76–79. <https://doi.org/10.1126/science.aay8060>
- 374 Bates, D., Maechler, M., Bolker, B.M., Walker, S., 2015. Fitting Linear Mixed-Effects Models Using lme4. *J.*
375 *Stat. Softw.* 67, 1–48. <https://doi.org/10.18637/jss.v067.i01>
- 376 Chen, J., Saunders, S.C., Crow, T.R., Naiman, R.J., Brosofske, K.D., Mroz, G.D., Brookshire, B.L., Franklin, J.F.,
377 1999. Microclimate in forest ecosystem and landscape ecology: Variations in local climate can be used
378 to monitor and compare the effects of different management regimes. *Bioscience* 49, 288–297.
379 <https://doi.org/10.2307/1313612>
- 380 Chen, Y., Liu, Y., Zhang, J., Yang, W., He, R., Deng, C., 2018. Microclimate exerts greater control over litter
381 decomposition and enzyme activity than litter quality in an alpine forest-tundra ecotone. *Sci. Rep.* 8,
382 1–13. <https://doi.org/10.1038/s41598-018-33186-4>
- 383 Curtis, P.G., Slay, C.M., Harris, N.L., Tyukavina, A., Hansen, M.C., 2018. Classifying drivers of global forest
384 loss. *Science* (80-). 361, 1108–1111. <https://doi.org/10.1126/science.aau3445>
- 385 Davis, K.T., Dobrowski, S.Z., Holden, Z.A., Higuera, P.E., Abatzoglou, J.T., 2019. Microclimatic buffering in
386 forests of the future: the role of local water balance. *Ecography* (Cop.). 42, 1–11.
387 <https://doi.org/10.1111/ecog.03836>
- 388 De Frenne, P., Lenoir, J., Luoto, M., Scheffers, B.R., Zellweger, F., Aalto, J., Ashcroft, M.B., Christiansen,
389 D.M., Decocq, G., Pauw, K. De, Govaert, S., Greiser, C., Gril, E., Hampe, A., Jucker, T., Klinges, D.H.,
390 Koelemeijer, I.A., Lembrechts, J.J., Marrec, R., Meeussen, C., Ogée, J., Tyystjärvi, V., Vangansbeke, P.,
391 Hylander, K., 2021. Forest microclimates and climate change : Importance, drivers and future research
392 agenda. *Glob. Chang. Biol.* 1–19. <https://doi.org/10.1111/gcb.15569>
- 393 de Frenne, P., Lenoir, J., Rodriguez-Sanchez, F., 2019. Global buffering of temperatures under forest
394 canopies data and code. *Figshare*. <https://doi.org/10.6084/m9.figshare.7604849tem>
- 395 De Frenne, P., Rodríguez-Sánchez, F., Coomes, D.A., Baeten, L., Verstraeten, G., Vellend, M., Bernhardt-
396 Römermann, M., Brown, C.D., Brunet, J., Cornelis, J., Decocq, G.M., Dierschke, H., Eriksson, O., Gilliam,
397 F.S., Hédli, R., Heinken, T., Hermy, M., Hommel, P., Jenkins, M. a, Kelly, D.L., Kirby, K.J., Mitchell, F.J.G.,
398 Naaf, T., Newman, M., Peterken, G., Petřík, P., Schultz, J., Sonnier, G., Van Calster, H., Waller, D.M.,
399 Walther, G.-R., White, P.S., Woods, K.D., Wulf, M., Graae, B.J., Verheyen, K., 2013. Microclimate
400 moderates plant responses to macroclimate warming. *Proc. Natl. Acad. Sci. U. S. A.* 110, 18561–
401 18565. <https://doi.org/10.1073/pnas.1311190110>
- 402 De Frenne, P., Zellweger, F., Rodríguez-Sánchez, F., Scheffers, B.R., Hylander, K., Luoto, M., Vellend, M.,
403 Verheyen, K., Lenoir, J., 2019. Global buffering of temperatures under forest canopies. *Nat. Ecol. Evol.*
404 3, 744–749. <https://doi.org/10.1038/s41559-019-0842-1>
- 405 De Smedt, P., Boeraeve, P., Baeten, L., 2021. Intra-annual activity patterns of terrestrial isopods are

406 tempered in forest compared to open habitat. *Soil Biol. Biochem.* 160, 108342.
407 <https://doi.org/10.1016/j.soilbio.2021.108342>

408 Di Sacco, A., Hardwick, K.A., Blakesley, D., Brancalion, P.H.S., Breman, E., Cecilio Rebola, L., Chomba, S.,
409 Dixon, K., Elliott, S., Ruyonga, G., Shaw, K., Smith, P., Smith, R.J., Antonelli, A., 2021. Ten golden rules
410 for reforestation to optimize carbon sequestration, biodiversity recovery and livelihood benefits. *Glob.*
411 *Chang. Biol.* 27, 1328–1348. <https://doi.org/10.1111/gcb.15498>

412 Dietz, L., Collet, C., Dupouey, J.L., Lacombe, E., Laurent, L., Gégout, J.C., 2020. Windstorm-induced canopy
413 openings accelerate temperate forest adaptation to global warming. *Glob. Ecol. Biogeogr.* 2067–2077.
414 <https://doi.org/10.1111/geb.13177>

415 Fick, S.E., Hijmans, R.J., 2017. WorldClim 2: new 1-km spatial resolution climate surfaces for global land
416 areas. *Int. J. Climatol.* 37, 4302–4315. <https://doi.org/10.1002/joc.5086>

417 Findell, K.L., Berg, A., Gentine, P., Krasting, J.P., Lintner, B.R., Malyshev, S., Santanello, J.A., Shevliakova, E.,
418 2017. The impact of anthropogenic land use and land cover change on regional climate extremes. *Nat.*
419 *Commun.* 8, 1–9. <https://doi.org/10.1038/s41467-017-01038-w>

420 Frey, S.J.K., Hadley, A.S., Betts, M.G., 2016a. Microclimate predicts within-season distribution dynamics of
421 montane forest birds. *Divers. Distrib.* 22, 944–959. <https://doi.org/10.1111/ddi.12456>

422 Frey, S.J.K., Hadley, A.S., Johnson, S.L., Schulze, M., Jones, J.A., Betts, M.G., 2016b. Spatial models reveal the
423 microclimatic buffering capacity of old-growth forests. *Sci. Adv.* 2.
424 <https://doi.org/10.1126/sciadv.1501392>

425 Geiger, R., Aron, R., Todhunter, P., 2009. *The climate near the ground.* Rowman & Littlefield.

426 Greiser, C., Meineri, E., Luoto, M., Ehrlén, J., Hylander, K., 2018. Monthly microclimate models in a
427 managed boreal forest landscape. *Agric. For. Meteorol.* 250–251, 147–158.
428 <https://doi.org/10.1016/j.agrformet.2017.12.252>

429 Haesen, S., Lembrechts, J.J., De Frenne, P., Lenoir, J., Aalto, J., Ashcroft, M.B., Kopecký, M., Luoto, M.,
430 Maclean, I., Nijs, I., Niittynen, P., Hoogen, J., Arriga, N., Brůna, J., Buchmann, N., Čiliak, M., Collalti, A.,
431 De Lombaerde, E., Descombes, P., Gharun, M., Goded, I., Govaert, S., Greiser, C., Grelle, A., Gruening,
432 C., Hederová, L., Hylander, K., Kreyling, J., Kruijt, B., Macek, M., Máliš, F., Man, M., Manca, G., Matula,
433 R., Meeussen, C., Merinero, S., Minerbi, S., Montagnani, L., Muffler, L., Ogaya, R., Penuelas, J., Plichta,
434 R., Portillo-Estrada, M., Schmeddes, J., Shekhar, A., Spicher, F., Ujházyová, M., Vangansbeke, P.,
435 Weigel, R., Wild, J., Zellweger, F., Van Meerbeek, K., 2021. ForestTemp – Sub-canopy microclimate
436 temperatures of European forests. *Glob. Chang. Biol.* 1–13. <https://doi.org/10.1111/gcb.15892>

437 Hansen, M.C., Potapov, P. V., Moore, R., Hancher, M., Turubanova, S.A., Tyukavina, A., Thau, D., Stehman, S.
438 V., Goetz, S.J., Loveland, T.R., Kommareddy, A., Egorov, A., Chini, L., Justice, C.O., Townshend, J.R.G.,
439 2013. High-Resolution Global Maps of 21st-Century Forest Cover Change. *Science* (80-). 342, 850–
440 854. <https://doi.org/10.1126/science.1244693>

441 Hijmans, R.J., van Etten, J., 2012. *raster: Geographic analysis and modeling with raster data.*

442 IPCC, 2018. *Global Warming of 1.5 °C - SR15 - Summary for Policy Makers, IPCC Climate Change Synthesis*
443 *Report.*

444 Lembrechts, J.J., Aalto, J., Ashcroft, M.B., De Frenne, P., Kopecký, M., Lenoir, J., Luoto, M., Maclean, I.M.D.,
445 Roupsard, O., Fuentes-Lillo, E., García, R.A., Pellissier, L., Pitteloud, C., Alatalo, J.M., Smith, S.W., Björk,
446 R.G., Muffler, L., Ratier Backes, A., Cesarz, S., Gottschall, F., Okello, J., Urban, J., Plichta, R., Svátek, M.,
447 Phartyal, S.S., Wipf, S., Eisenhauer, N., Puşcaş, M., Turtureanu, P.D., Varlagin, A., Dimarco, R.D., Jump,
448 A.S., Randall, K., Dorrepaal, E., Larson, K., Walz, J., Vitale, L., Svoboda, M., Finger Higgens, R.,
449 Halbritter, A.H., Curasi, S.R., Klupar, I., Koontz, A., Pearce, W.D., Simpson, E., Stemkovski, M., Jessen
450 Graae, B., Vedel Sørensen, M., Høye, T.T., Fernández Calzado, M.R., Lorite, J., Carbognani, M.,
451 Tomaselli, M., Forte, T.G.W., Petraglia, A., Haesen, S., Somers, B., Van Meerbeek, K., Björkman, M.P.,

452 Hylander, K., Merinero, S., Gharun, M., Buchmann, N., Dolezal, J., Matula, R., Thomas, A.D., Bailey, J.J.,
453 Ghosn, D., Kazakis, G., de Pablo, M.A., Kemppinen, J., Niittynen, P., Rew, L., Seipel, T., Larson, C.,
454 Speed, J.D.M., Ardö, J., Cannone, N., Guglielmin, M., Malfasi, F., Bader, M.Y., Canessa, R., Stanisci, A.,
455 Kreyling, J., Schmeddes, J., Teuber, L., Aschero, V., Čiliak, M., Máliš, F., De Smedt, P., Govaert, S.,
456 Meeussen, C., Vangansbeke, P., Gigauri, K., Lamprecht, A., Pauli, H., Steinbauer, K., Winkler, M.,
457 Ueyama, M., Nuñez, M.A., Ursu, T.M., Haider, S., Wedegärtner, R.E.M., Smiljanic, M., Trouillier, M.,
458 Wilmking, M., Altman, J., Brůna, J., Hederová, L., Macek, M., Man, M., Wild, J., Vittoz, P., Pärtel, M.,
459 Barančok, P., Kanka, R., Kollár, J., Palaj, A., Barros, A., Mazzolari, A.C., Bauters, M., Boeckx, P., Benito
460 Alonso, J.L., Zong, S., Di Cecco, V., Sitková, Z., Tielbörger, K., van den Brink, L., Weigel, R., Homeier, J.,
461 Dahlberg, C.J., Medinets, S., Medinets, V., De Boeck, H.J., Portillo-Estrada, M., Verryckt, L.T., Milbau,
462 A., Daskalova, G.N., Thomas, H.J.D., Myers-Smith, I.H., Blonder, B., Stephan, J.G., Descombes, P.,
463 Zellweger, F., Frei, E.R., Heinesch, B., Andrews, C., Dick, J., Siebicke, L., Rocha, A., Senior, R.A., Rixen,
464 C., Jimenez, J.J., Boike, J., Pauchard, A., Scholten, T., Scheffers, B., Klinges, D., Basham, E.W., Zhang, J.,
465 Zhang, Z., Géron, C., Fazlioglu, F., Candan, O., Sallo Bravo, J., Hrbacek, F., Laska, K., Cremonese, E.,
466 Haase, P., Moyano, F.E., Rossi, C., Nijs, I., 2020. SoilTemp: A global database of near-surface
467 temperature. *Glob. Chang. Biol.* 26, 6616–6629. <https://doi.org/10.1111/gcb.15123>

468 Lembrechts, J.J., Hoogen, J. Van Den, Aalto, J., Ashcroft, M.B., De Frenne, P., Kemppinen, J., Kopecký, M.,
469 2021a. Mismatches between soil and air temperature. *EcoEvoRxiv*.
470 <https://doi.org/10.32942/osf.io/pksqw>

471 Lembrechts, J.J., Lenoir, J., Frenne, P. De, Scheffers, B.R., 2021b. Designing countrywide and regional
472 microclimate networks 1–7. <https://doi.org/10.1111/geb.13290>

473 Lembrechts, J.J., Nijs, I., 2020. Microclimate shifts in a dynamic world. *Science* (80-). 368, 711–712.

474 Lembrechts, J.J., Nijs, I., Lenoir, J., 2019. Incorporating microclimate into species distribution models.
475 *Ecography (Cop.)*. 42, 1267–1279. <https://doi.org/10.1111/ecog.03947>

476 Lenoir, J., Hattab, T., Pierre, G., 2017. Climatic microrefugia under anthropogenic climate change:
477 implications for species redistribution. *Ecography (Cop.)*. 40, 253–266.
478 <https://doi.org/10.1111/ecog.02788>

479 Li, Y., Zhao, M., Motesharrei, S., Mu, Q., Kalnay, E., Li, S., 2015. Local cooling and warming effects of forests
480 based on satellite observations. *Nat. Commun.* 6. <https://doi.org/10.1038/ncomms7603>

481 Macek, M., Kopecký, M., Wild, J., 2019. Maximum air temperature controlled by landscape topography
482 affects plant species composition in temperate forests. *Landsc. Ecol.* 34, 2541–2556.
483 <https://doi.org/10.1007/s10980-019-00903-x>

484 Maclean, I.M.D., Suggitt, A.J., Wilson, R.J., Duffy, J.P., Bennie, J.J., 2017. Fine-scale climate change:
485 modelling spatial variation in biologically meaningful rates of warming. *Glob. Chang. Biol.* 23, 256–
486 268. <https://doi.org/10.1111/gcb.13343>

487 Nakagawa, S., Schielzeth, H., 2013. A general and simple method for obtaining R² from generalized linear
488 mixed-effects models. *Methods Ecol. Evol.* 4, 133–142. [https://doi.org/10.1111/j.2041-
489 210x.2012.00261.x](https://doi.org/10.1111/j.2041-210x.2012.00261.x)

490 Olson, D.M., Dinerstein, E., Wikramanayake, E.D., Burgess, N.D., Powell, G.V.N., Underwood, E.C., Amico,
491 J.A.D., Itoua, I., Strand, H.E., Morrison, J.C., Loucks, J., Allnutt, T.F., Ricketts, T.H., Kura, Y., Lamoreux,
492 J.F., Wesley, W., Hedao, P., Kassem, K.R., 2001. *Terrestrial Ecoregions of the World : A New Map of
493 Life on Earth* 51, 933–938.

494 Paradis, E., Schliep, K., 2019. Ape 5.0: An environment for modern phylogenetics and evolutionary analyses
495 in R. *Bioinformatics* 35, 526–528. <https://doi.org/10.1093/bioinformatics/bty633>

496 R Core Team, 2021. R: A language and environment for statistical computing.

497 Randin, C.F., Ashcroft, M.B., Bolliger, J., Cavender-Bares, J., Coops, N.C., Dullinger, S., Dirnböck, T., Eckert,

498 S., Ellis, E., Fernández, N., Giuliani, G., Guisan, A., Jetz, W., Joost, S., Karger, D., Lembrechts, J., Lenoir,
499 J., Luoto, M., Morin, X., Price, B., Rocchini, D., Schaeppman, M., Schmid, B., Verburg, P., Wilson, A.,
500 Woodcock, P., Yoccoz, N., Payne, D., 2020. Monitoring biodiversity in the Anthropocene using remote
501 sensing in species distribution models. *Remote Sens. Environ.* 239, 111626.
502 <https://doi.org/10.1016/j.rse.2019.111626>

503 Richard, B., Dupouey, J.L., Corcket, E., Alard, D., Archaux, F., Aubert, M., Boulanger, V., Gillet, F., Langlois, E.,
504 Macé, S., Montpied, P., Beaufils, T., Begeot, C., Behr, P., Boissier, J.M., Camaret, S., Chevalier, R.,
505 Decocq, G., Dumas, Y., Eynard-Machet, R., Gégout, J.C., Huet, S., Malécot, V., Margerie, P., Mouly, A.,
506 Paul, T., Renaux, B., Ruffaldi, P., Spicher, F., Thirion, E., Ulrich, E., Nicolas, M., Lenoir, J., 2021. The
507 climatic debt is growing in the understorey of temperate forests: Stand characteristics matter. *Glob.
508 Ecol. Biogeogr.* 30, 1474–1487. <https://doi.org/10.1111/geb.13312>

509 Sanderson, B.M., Knutti, R., Caldwell, P., 2015. A representative democracy to reduce interdependency in a
510 multimodel ensemble. *J. Clim.* 28, 5171–5194. <https://doi.org/10.1175/JCLI-D-14-00362.1>

511 Senf, C., Sebald, J., Seidl, R., 2021. Increasing canopy mortality affects the future demographic structure of
512 Europe's forests. *One Earth* 1–7. <https://doi.org/10.1016/j.oneear.2021.04.008>

513 Senf, C., Seidl, R., 2020. Mapping the forest disturbance regimes of Europe. *Nat. Sustain.*
514 <https://doi.org/10.1038/s41893-020-00609-y>

515 Simard, M., Pinto, N., Fisher, J.B., Baccini, A., 2011. Mapping forest canopy height globally with spaceborne
516 lidar. *J. Geophys. Res. Biogeosciences* 116, 1–12. <https://doi.org/10.1029/2011JG001708>

517 Stevens, J.T., Safford, H.D., Harrison, S., Latimer, A.M., 2015. Forest disturbance accelerates
518 thermophilization of understory plant communities. *J. Ecol.* 103, 1253–1263.
519 <https://doi.org/10.1111/1365-2745.12426>

520 Tennekes, M., 2018. Tmap: Thematic maps in R. *J. Stat. Softw.* 84. <https://doi.org/10.18637/jss.v084.i06>

521 Thrippleton, T., Bugmann, H., Kramer-Priewasser, K., Snell, R.S., 2016. Herbaceous Understorey : An
522 Overlooked Player in Forest Landscape Dynamics? *Ecosystems* 19, 1240–1254.
523 <https://doi.org/10.1007/s10021-016-9999-5>

524 Valavi, R., Elith, J., Lahoz-Monfort, J.J., Guillera-Arroita, G., 2019. blockCV: An r package for generating
525 spatially or environmentally separated folds for k-fold cross-validation of species distribution models.
526 *Methods Ecol. Evol.* 10, 225–232. <https://doi.org/10.1111/2041-210X.13107>

527 Von Arx, G., Graf Pannatier, E., Thimonier, A., Rebetez, M., 2013. Microclimate in forests with varying leaf
528 area index and soil moisture: Potential implications for seedling establishment in a changing climate. *J.
529 Ecol.* 101, 1201–1213. <https://doi.org/10.1111/1365-2745.12121>

530 Wickham, H., 2016. *ggplot2: elegant graphics for data analysis*. Springer, New York, USA.

531 Wolf, C., Bell, D.M., Kim, H., Paul, M., Schulze, M., Betts, M.G., Northwest, P., Service, U.F., Way, S.W.J., Or,
532 C., 2021. Temporal consistency of undercanopy thermal refugia in old-growth forest. *Agric. For.
533 Meteorol.* 307, 108520. <https://doi.org/10.1016/j.agrformet.2021.108520>

534 Wood, S., Scheipl, F., 2014. *gamm4: Generalized additive mixed models using mgcv and lme4*.

535 World Meteorological Organization, 2018. *Guide to meteorological instruments and methods of
536 observation, 2018 Editi. ed. WMO*.

537 Zellweger, F., Coomes, D., Lenoir, J., Depauw, L., Maes, S.L., Wulf, M., Kirby, K.J., Brunet, J., Kopecký, M.,
538 Máliš, F., Schmidt, W., Heinrichs, S., den Ouden, J., Jaroszewicz, B., Buyse, G., Spicher, F., Verheyen, K.,
539 De Frenne, P., 2019. Seasonal drivers of understorey temperature buffering in temperate deciduous
540 forests across Europe. *Glob. Ecol. Biogeogr.* 28, 1774–1786. <https://doi.org/10.1111/geb.12991>

541 Zellweger, F., De Frenne, P., Lenoir, J., Rocchini, D., Coomes, D., 2018. Advances in microclimate ecology

542 arising from remote sensing. *Trends Ecol. Evol.* xx, 1–15. <https://doi.org/10.1016/j.tree.2018.12.012>

543 Zellweger, F., De Frenne, P., Lenoir, J., Vangansbeke, P., Verheyen, K., Bernhardt-römermann, M., Baeten,
544 L., Hédli, R., Berki, I., Brunet, J., Van Calster, H., Chudomelov, 2020. Forest microclimate dynamics drive
545 plant responses to warming. *Science* (80-.). 368, 772–775.

546 Zuur, A.F., Ieno, E.N., Elphick, C.S., 2010. A protocol for data exploration to avoid common statistical
547 problems 3–14. <https://doi.org/10.1111/j.2041-210X.2009.00001.x>

548